# Power Quality Improvement with Harmonic Reduction Using P-Q Theory-Based Shunt Active Power Filter


**Kiran Yadav, Gitanjali Mehta, and Vinod Kumar Yadav**

**Abstract** The penetration of nonlinear loads is responsible for load-side harmonic current. Customer awareness about power quality issues has made it indispensable to analyze the effect of nonlinear and linear loads. The active filter has shown a number of advantages against passive filter due to impractical solutions and size problems associated with the passive filter. In this paper, Shunt Active Power Filter (SAPF) has been implemented with a P-Q theory-based control scheme. A compensating current is calculated by the controller which is fed to the shunt active filter. SAPF can be widely implemented in industrial applications. The objective is to eliminate unrequited harmonics so as to improve the voltage profile in the system. Simulation on MATLAB has been carried out to corroborate the results, and Total Harmonic Distortion (THD) is compared for varying loads.

**Keywords** Power quality · Shunt active power filter · P-Q theory · Harmonics · Total harmonic distortion

## 1 Introduction

For the past decades, electronics-based equipment has proliferated the consumer market. The most prominent of them is adjustable speed drives (ASDs) providing efficient output to the industry. However, it produces a significant change in the sinusoidal nature of voltage and current. Hence, attempts have been made to meet the challenge of using drives by a reduction in distortion [1, 2]. When an ASD is connected to the system, it is responsible for producing harmonic distortion. These ASDs draw non-sinusoidal current from the supply filled with harmonics which in turn flows into the system and distorts voltage and current waveform. This was noted

K. Yadav · G. Mehta (✉)
Electrical Engineering Department, Galgotias University, G. Noida, India
e-mail: gitanjali.iitr@gmail.com

V. K. Yadav
Electrical Engineering Department, Delhi Technological University, Delhi, India



K. Namrata et al. (eds.), *Smart Energy and Advancement in Power Technologies*,
Lecture Notes in Electrical Engineering 927,
https://doi.org/10.1007/978-981-19-4975-3_1

not only for ASDs but also for converter circuits, UPS and other AC-DC and DC-AC conversion systems. Thus, deviation of a waveform to non-sinusoidal is attributed to harmonics and distortion [3, 4]. Conditioning of load and conditioning of line are the two ways to address harmonic related issues. The latter comprises passive and active filter methodology. Resonance and distinct filter for each frequency limit the implementation of the passive filter. Therefore, active filters paved the way for cutting-edge solutions for voltage and current-related disturbances [5–7]. Control techniques employed in the system make it most suitable and in-demand industrial solution. Hence, active filter accomplishes harmonic limitation and reactive power compensation [8–12].

## 2 Active Power Filters

Conventionally, passive filters were used with the combination of inductor and capacitor [5]. Although they were low in cost and less complex in design, they were more prone to impact resonance and hence active filters were designed. Active filters generally employ IGBT or MOSFET to provide switching circuits [6]. Figures 1, 2 and 3 depict the general active filter mechanism in use. The controller is shown with only one gate signal. In all the cases, an internal goto signal is used in MATLAB to provide current information which is used to generate a compensating current in the system.

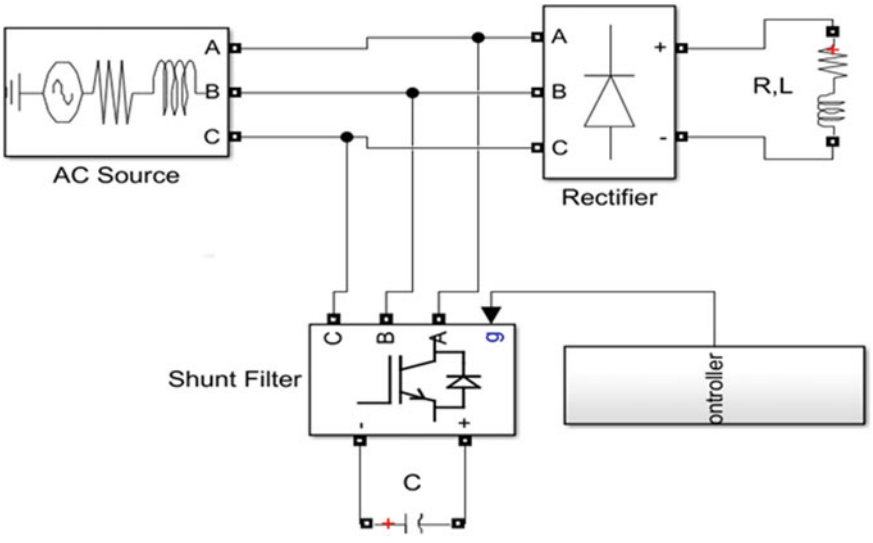


**Fig. 1** SAPF circuit diagram

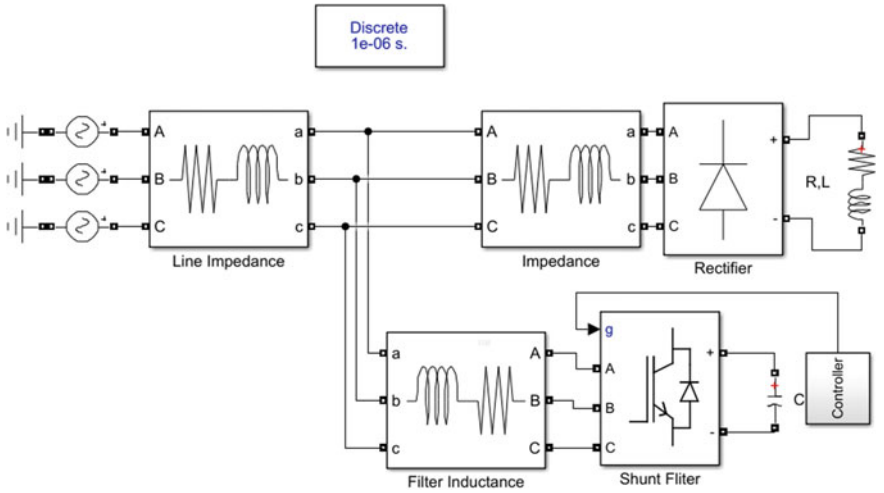


**Fig. 2** SAPF being used as voltage source

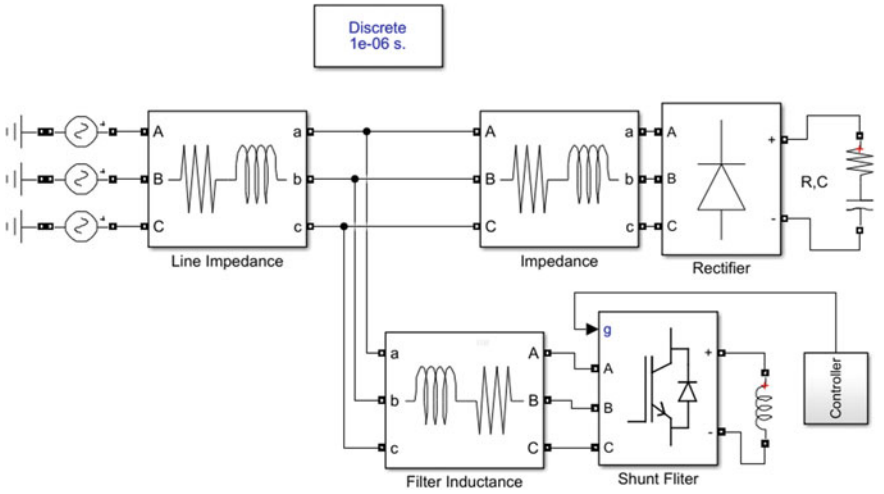


**Fig. 3** SAPF being used as current source

In this, a rectifier is connected across linear or nonlinear load which converts AC-DC and hence harmonic generation from the load side. A parallel active filter is connected which gives compensating current based on controller and therefore prevents harmonic current to reach AC source. In this way, the harmonic current is prevented to distort the source voltage. Active filters are dynamic in nature. They can be used as a current source and voltage source. Figure 2 shows when a filter is used as a voltage source connected with a capacitor and Fig. 3 depicts when a filter

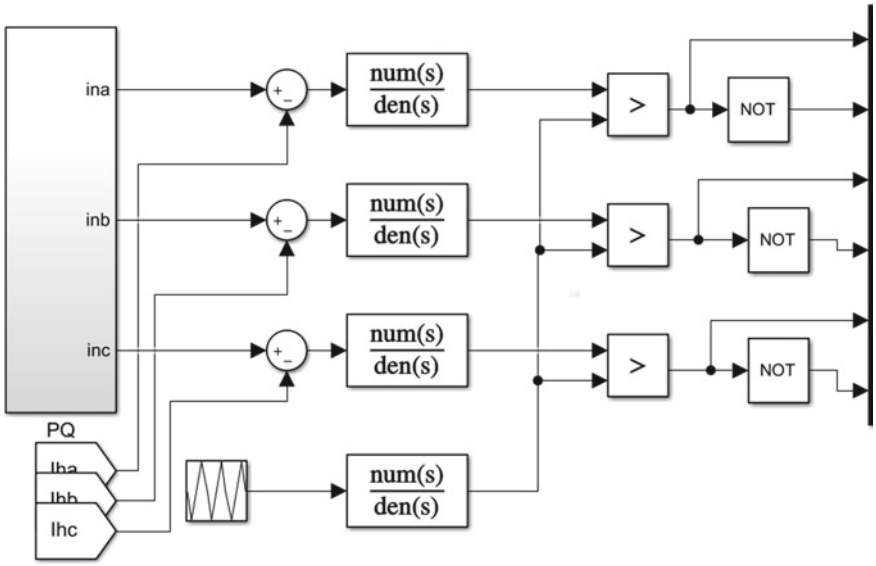


**Fig. 4** Control scheme based on P-Q theory

is used as a current source connected with an inductor. Passive filter topologies are shunt LC and shunt low pass filter. Active filter topologies are series, shunt and a combination of series-shunt called hybrid [7]. Active filter offers the convenience of configuration for over current in system and can result in less harmonics with an increase in frequency component. Figure 4 shows the control scheme based on instantaneous P-Q theory.

## 3 Instantaneous P-Q Power Theory

The P-Q theory also referred to as instantaneous power theory is based on Clarke and Parke transformations. In Clarke transformation, voltages and current for a three-phase system are reconstructed in terms of α and β [8].

$$i_{\alpha\beta o} = \sqrt{2/3}\begin{bmatrix} 1 & -1/2 & -1/2 \\ 0 & \sqrt{3}/2 & -\sqrt{3}/2 \\ 1/\sqrt{2} & 1/\sqrt{2} & 1/\sqrt{2} \end{bmatrix} i_{abc} \tag{1}$$

$$v_{\alpha\beta o} = \sqrt{2/3}\begin{bmatrix} 1 & -1/2 & -1/2 \\ 0 & \sqrt{3}/2 & -\sqrt{3}/2 \\ 1/\sqrt{2} & 1/\sqrt{2} & 1/\sqrt{2} \end{bmatrix} v_{abc} \tag{2}$$

Here, $i_{abc}$ is the three-phase source current and $v_{abc}$ is the three-phase source voltage of the system. Similarly, active and reactive power components are represented. Equation 3 represents instantaneous real power and Eq. 4 represents instantaneous imaginary power where voltage and current are represented in terms of a-b-c coordinates and $\alpha$-$\beta$ coordinates.

$$p = v_\alpha i_\alpha + v_\beta i_\beta \tag{3}$$

$$q = v_\alpha i_\beta - v_\beta i_\alpha \tag{4}$$

In matrix form, the above equation is represented as

$$\begin{bmatrix} p \\ q \end{bmatrix} = \begin{bmatrix} v_\alpha & v_\beta \\ -v_\beta & v_\alpha \end{bmatrix} \begin{bmatrix} i_\alpha \\ i_\beta \end{bmatrix} \tag{5}$$

Then, active and reactive power is divided into AC and DC components. A low pass filter is connected across the circuit to obtain the DC component of both active and reactive power.

$$p = \overline{p} + \tilde{q} \tag{6}$$

$$q = \overline{q} + \tilde{p} \tag{7}$$

The P-Q theory states that the DC component of active power is represented in terms of α and β reference current as

$$i^*_{\alpha\beta} = \frac{1}{v_\alpha^2 + v_\beta^2} \begin{bmatrix} v_\alpha & v_\beta \\ -v_\beta & v_\alpha \end{bmatrix} \begin{bmatrix} p \\ q \end{bmatrix} \tag{8}$$

And thus, the reference current is given as

$$i^*_{\alpha\beta} = \sqrt{2}/3 \begin{bmatrix} 1 & 0 \\ -1/2 & \sqrt{3}/2 \\ -1/\sqrt{2} & -\sqrt{3}/2 \end{bmatrix} i^*_{\alpha\beta} \tag{9}$$

## 4 Simulation Results and Discussion

Shunt active power filter circuit for simulation is shown in Fig. 5. Figure 6 shows the P-Q controller for shunt APF simulation. The authors have calculated THD under three different load conditions. In the first case, RL load is considered connected

to the DC side of the rectifier. Figures 7, 8, 9, 10, 11 and 12 depict waveforms for rectifier with RL load. In Fig. 7, source voltage of all three phases is depicted. In Fig. 8, source current is depicted in phase-a. In Fig. 9 load current is depicted. In Fig. 10 compensating current is depicted. In Fig. 11 THD for load current is depicted which is 24.49%. In Fig. 12, THD for source current is depicted which comes out to be 5.44%. In the second case, RC load is connected to the DC side of the rectifier. THD in source current for this came out to be 6.44%. Figures 13, 14, 15 and 16 show waveforms for rectifiers with RC load. Figure 13 shows the source current and in Fig. 14 load current is shown. In Fig. 15, THD for load current is depicted which is 22.49%. In Fig. 16, THD for source current is depicted which is 6.44%. And, in the third case R load is connected to the DC side of the rectifier. THD of source current comes out to be 10.27%. Waveforms from Figs. 17, 18, 19 and 20 are shown for rectifier with R load. In Fig. 17 source current is depicted. In Fig. 18 load current is shown. In Fig. 19, THD for load current is depicted which is 21.64%, and in Fig. 20 THD for source current is depicted which is 10.27%. Table 1 shows the parameters and their values. Table 2 shows order-wise source current harmonics with rectifier R-L load using SAPF. Table 3 shows the THD values of load current and source currents for different types of rectifier loads (Fig. 21).

## 5 Conclusion

Shunt active filter is implemented using a P-Q theory-based controller in this paper. SAPF has been able to mitigate harmonic components present in the source current due to the rectifier which is a nonlinear load. A control mechanism is used to provide compensating current in the system so as to maintain the source current sinusoidal. THDs obtained through FFT analysis for different loads conclude that THD in source current is considerably reduced for all three loads. MATLAB simulation has been carried out in order to inspect the waveforms and their THD components associated with them. Tabular representation is also provided for different loads to analyze its effect.

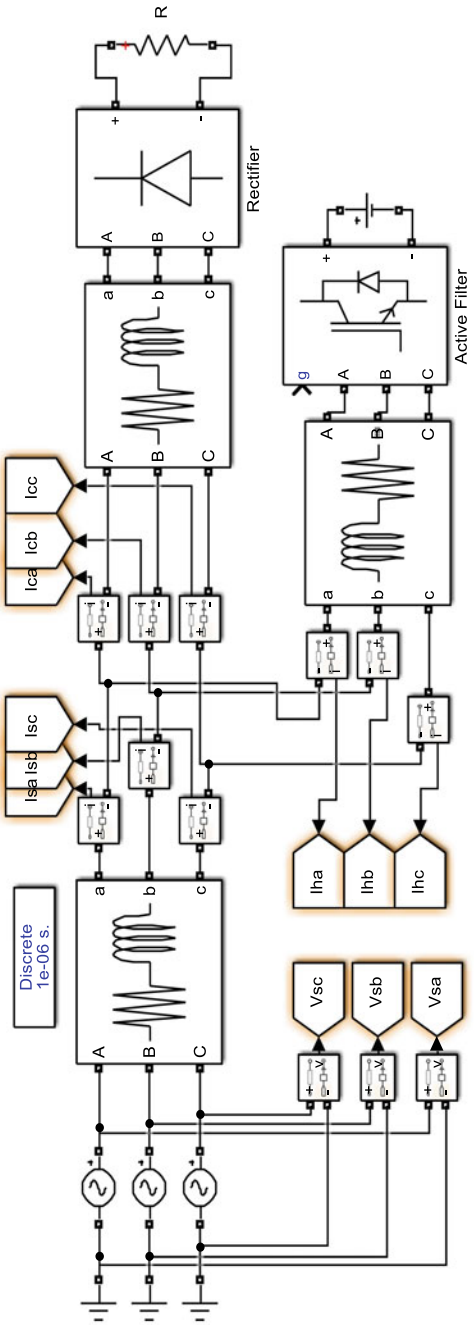


**Fig. 5** Shunt APF showing Rectifier with *R* load

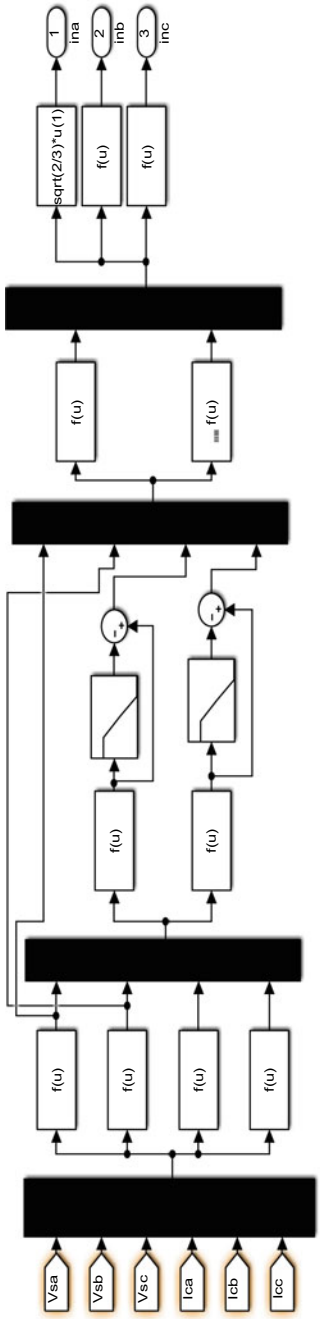


**Fig. 6** P-Q controller for Shunt APF

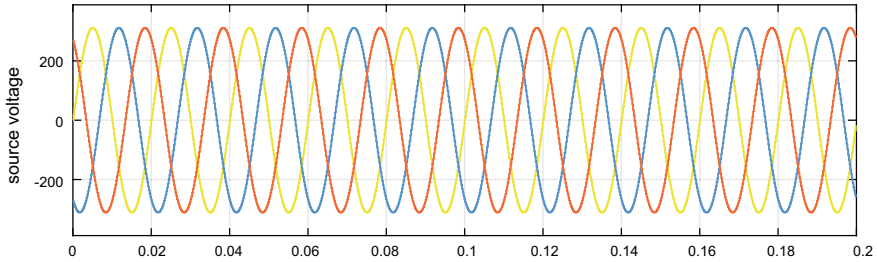


**Fig. 7** Three-phase source voltage for RL load

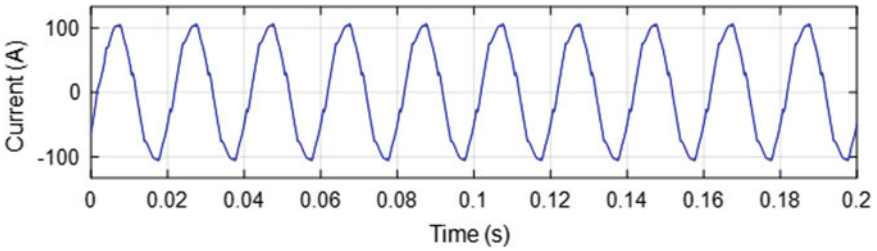


**Fig. 8** Source current for RL load

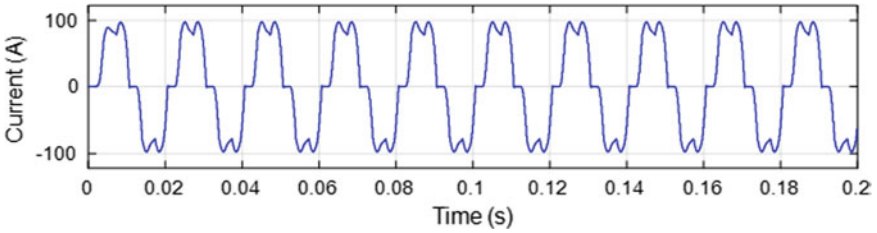


**Fig. 9** Load current for RL load

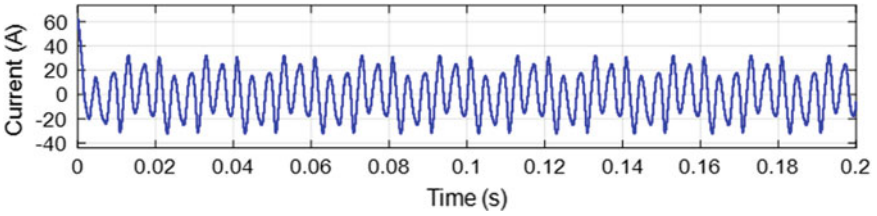


**Fig. 10** Compensating current for RL load

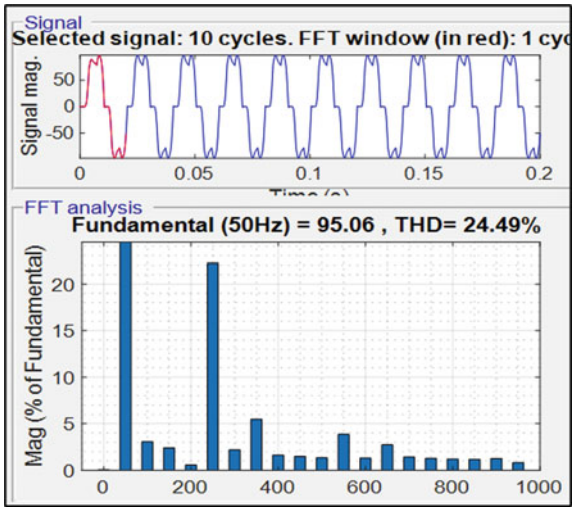


**Fig. 11** THD for load current with RL load

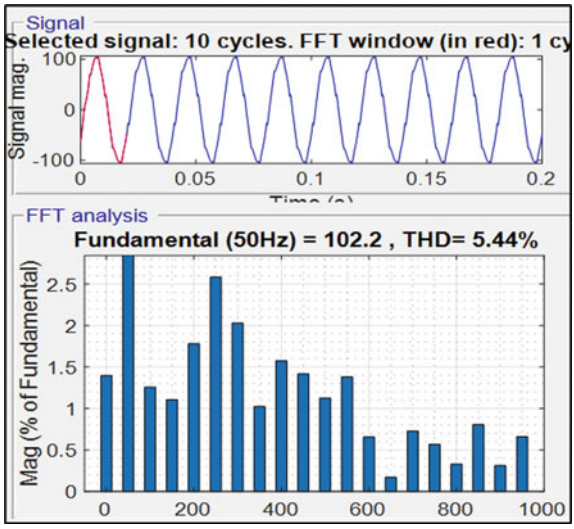


**Fig. 12** THD for source current with RL load

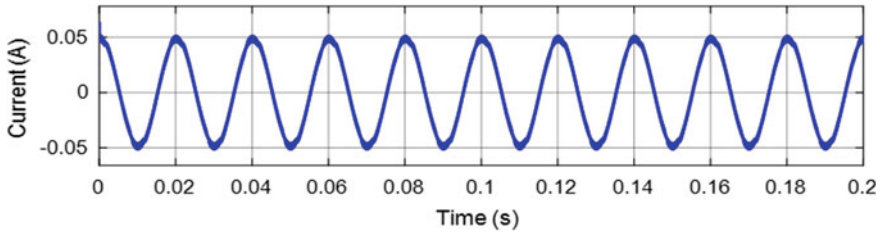


**Fig. 13** Source current for RC load

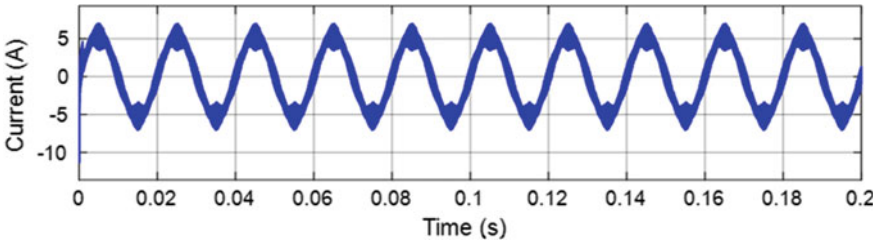


**Fig. 14** Load current for RC load

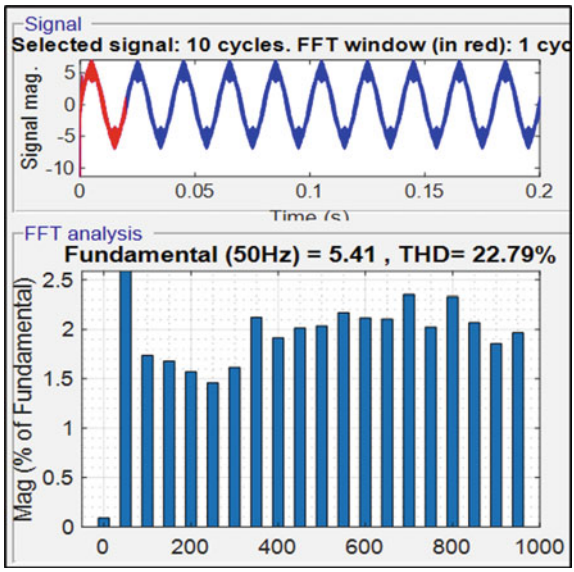


**Fig. 15** THD for load current with RC load

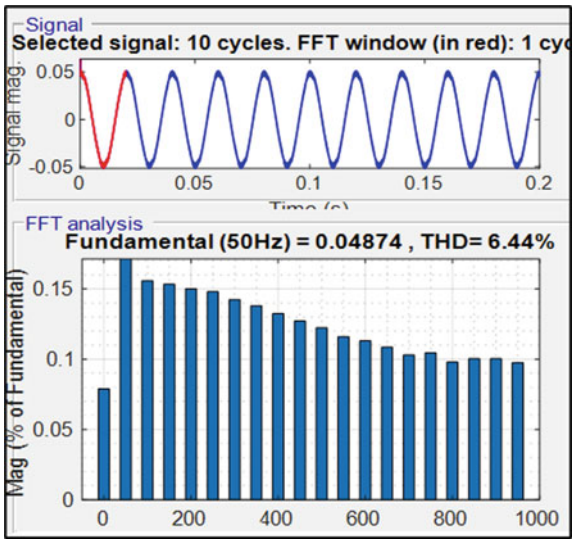


**Fig. 16** THD for source current with RC load

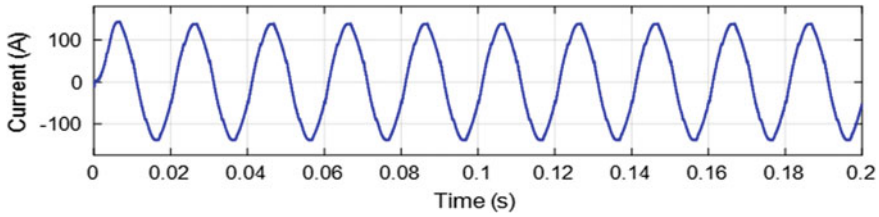


**Fig. 17** Source current for R load

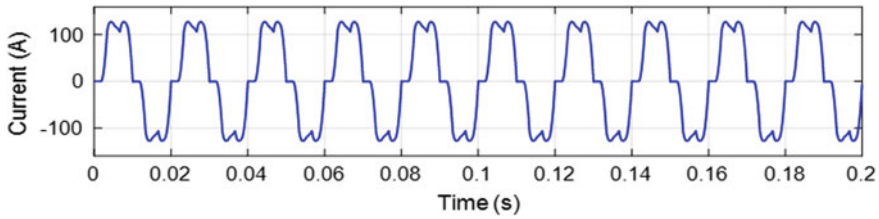


**Fig. 18** Load current for R load

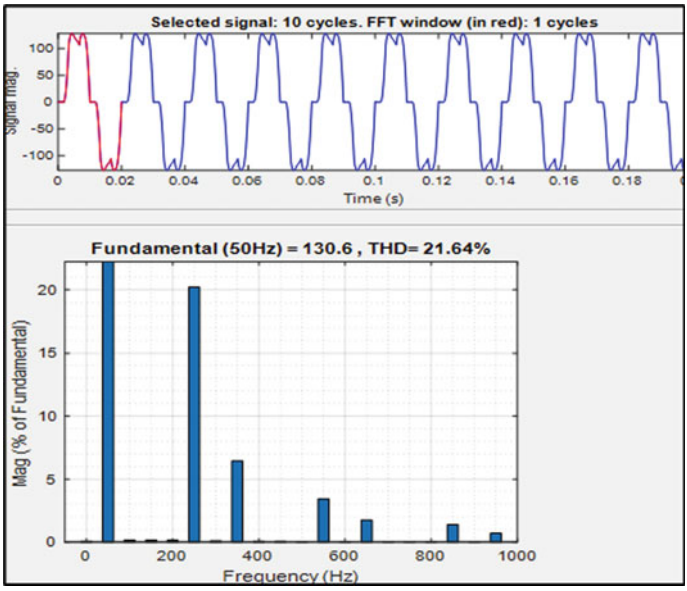


**Fig. 19** THD for load current with R load

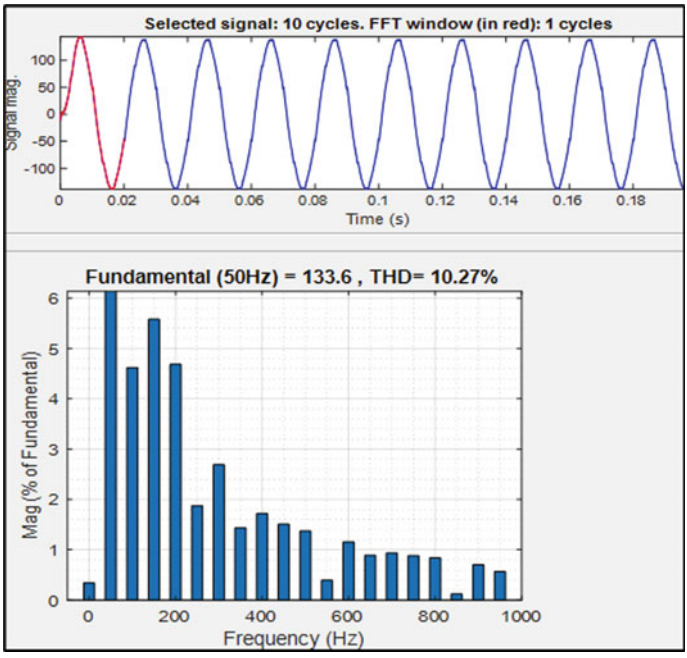


**Fig. 20** THD for source current with R load

**Table 1** Parameter values

| Parameter | Value |
|---|---|
| Source voltage, frequency | 310 V, 50 Hz |
| Source impedance | $R = 0.2\ \Omega\ L = 0.16$ mH |
| DC link voltage $V_{dc}$ | 840 V |
| Filter inductor $L_c$ | 3 mH |
| RL load | $R = 6.2\ \Omega L = 20$ mH |
| R load | $R = 6.2\ \Omega$ |
| RC load | $R = 15\ \Omega\ C = 8\ \mu$F |

**Table 2** Harmonic components in source current for Rectifier RL load

| Harmonic order | % Value |
|---|---|
| 3rd | 3.82 |
| 5th | 1.1 |
| 7th | 0.6 |
| 9th | 0.43 |
| 11th | 0.40 |
| 13th | 0.3 |
| 15th | 0.1 |
| 17th | 0.3 |
| 19th | 0.2 |
| THD % | 5.44 |

**Table 3** Computation of THD

| Load | Source current (%) | Load current (%) |
|---|---|---|
| Rectifier with R, L load | 24.49 | 5.44 |
| Rectifier with R load | 21.64 | 10.27 |
| Rectifier with R, C load | 22.49 | 6.44 |

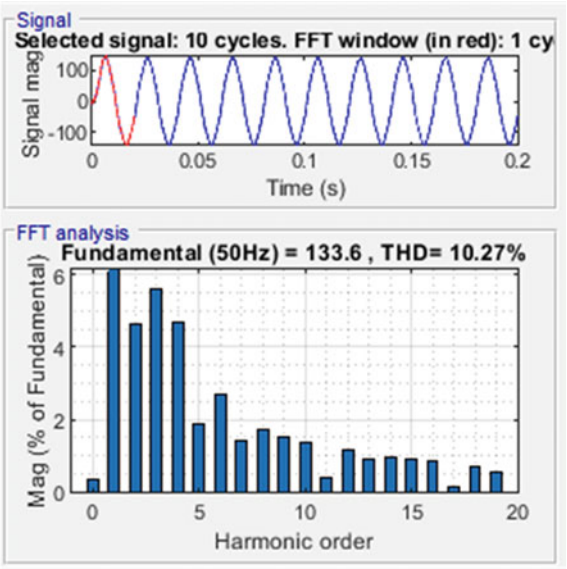


**Fig. 21** THD for source current with R load harmonic order

## References


1. Bhattacharya S, Frank TM, Divan DM, Banerjee B (1998) Active filter system implementation. IEEE Ind Appl Mag 4(5):47–63
2. Hoevenaars T, LeDoux K, Colosino M (2003) Interpreting IEEE STD 519 and meeting its harmonic limits in VFD applications. In: IEEE industry applications society 50th annual petroleum and chemical industry conference, Houston, TX, USA, pp 145–150
3. Mehta G, Singh SP (2013) Power quality improvement through grid integration of renewable energy sources. IETE J Res 59(3):210–218
4. Mehta G, Singh SP (2013) Improvement of power quality at PCC through grid interfacing photovoltaic system. In: Proceedings of the sixth IASTED Asian conference on power and energy systems AsiaPES, Phuket, Thailand
5. Mehta G, Singh SP, Patidar RD (2013) Fuel cell based distributed generation system with power flow and power quality control. Int J Power Energy Conversion 4(1):73–94
6. Nie X, Liu J (2019) Current reference control for shunt active power filters under unbalanced and distorted supply voltage conditions. IEEE Access 7:177048–177055
7. Mehta G, Patidar RD, Singh SP (2011) Design, analysis and implementation of DSP based single-phase shunt active filter controller. In: Proceedings of IEEE international conference on emerging trends in electrical and computer technology, India, pp 166–173
8. Lada MY, Bugis I, Talib MHN (2010) Simulation a shunt active power filter using MATLAB/Simulink. In: International power engineering and optimization conference, Shah Alam, pp 371–375
9. Yadav VK, Mehta G, Kumari R, Patidar RD (2016) Power quality improvement using D-STATCOM and DVR. In: Proceedings of 2nd international conference on advances in steel, power and construction technology, O. P. Jindal University, Raigarh, Chhattisgarh, India
10. Amerise A, Mengoni M, Rizzoli G, Zarri L, Tani A, Casadei D (2020) Comparison of three voltage saturation algorithms in shunt active power filters with selective harmonic control. IEEE Trans Ind Appl 56(3):2762–2772

11. Meloni LFJ, Tofoli FL, Rezek AJJ, Ribeiro ER (2019) Modeling and experimental validation of a single-phase series active power filter for harmonic voltage reduction. IEEE Access 7:151971–151984
12. Devassy S, Singh B (2019) Implementation of solar photovoltaic system with universal active filtering capability. IEEE Trans Ind Appl 55(4):3926–3934